




ORIGINAL RESEARCH

Characterizing oceanographic conditions near Coiba Island and Pacific Panama using 20 years of satellite-based wind stress, SST and chlorophyll-*a* measurements

GREG CRAWFORD^{1,2,*}, MATTHEW MEPSTEAD¹ and EDGARDO DÍAZ-FERGUSON^{2,*}

¹Ontario Tech University, L1G 0C5 - Oshawa, Canada. ²Estación Científica Coiba (COIBA AIP), Calle Gustavo Lara, Edificio 145B, Ciudad del Saber, 0843-01853 - Clayton, Panamá. ORCID *Greg Crawford*  <https://orcid.org/0000-0003-3194-4576>, *Matthew Mepstead*  <https://orcid.org/0009-0007-9966-7604>, *Edgardo Díaz-Ferguson*  <https://orcid.org/0000-0002-2314-5021>



*Correspondence:
greg.crawford@ontariotechu.ca (GC)
ediaz@coiba.org.pa (EDF)

Received: 21 June 2023
Accepted: 30 October 2023

ISSN 2683-7595 (print)
ISSN 2683-7951 (online)

<https://ojs.inidep.edu.ar>

Journal of the Instituto Nacional de
Investigación y Desarrollo Pesquero
(INIDEP)



This work is licensed under a Creative
Commons Attribution-
NonCommercial-ShareAlike 4.0
International License

ABSTRACT. Coiba Island and the associated Special Zone of Marine Protection represent an important, yet poorly studied marine reserve along the Pacific coast of Panama. While efforts have recently began to establish monitoring programs in the region, a range of historical, marine-related environmental measurements already exist, derived from satellite-based observations. The goal of this paper was to use long-term datasets for key variables to provide qualitative insights (i.e. descriptive oceanography) of climatological conditions and interannual variability in the Pacific Panama region. These are underpinned with numerical assessments, providing an important baseline for ongoing and future studies, particularly in the Coiba Island/Gulf of Chiriqui region. In particular, we examined 20 years (January 2003-December 2022) of wind stress, sea surface temperature (SST), and chlorophyll-*a* (Chl-*a*), spanning the neritic and pelagic regions of the Pacific Panama coast. During the dry season (northern winter), the well-known, seasonal, regional Panama wind jet appeared across the Gulf of Panama, leading to surface mixing and SST cooling that eventually extended across most of the Panama Bight. West of the Azuero Peninsula, SST increased and surface warming extended further offshore from January through April. The SST in the Gulf of Chiriqui during this period was about 1 °C warmer on average than east of Coiba Island. By July and August, offshore SST gradients became largely longitudinal, cooling occurred across the season, and the SST on either side of Coiba Island was nearly the same. The influence of the Panama jet in the Gulf of Panama was clear in the Chl-*a* data as well, with upwelling-driven values peaking in February/March (up to 11 mg m⁻³, with a monthly climatological value of around 2 mg m⁻³ during this period). During the rest of the year, the Chl-*a* concentration in this region averaged around 0.5-1.0 mg m⁻³. In the Gulf of Chiriqui and the region east of Coiba Island, the climatological monthly averages were roughly 0.3-0.5 mg m⁻³ and 0.4-0.6 mg m⁻³, respectively. Somewhat surprisingly, very high Chl-*a* values were present in the satellite data for the Gulf of Chiriqui during May 2007 and June 2008, peaking at 16 mg m⁻³ and 32 mg m⁻³ at a location just west of Coiba Island, respectively. It remains unclear as to the cause of these apparent blooms. Even when the high Chl-*a* values were excluded in the calculation of climatological averages in the Gulf of Chiriqui, however, there is a suggestion of modest seasonality in Chl-*a* values, with slightly elevated values (~ 0.4 mg m⁻³) peaking around May and October. During the extreme El Niño event of 2015-2016, the monthly-averaged SST along the Panama Pacific coast was warmer than average, with elevated levels of up to + 2 °C and lasting 12 months in the Gulf of Chiriqui. In the Gulf of Panama, the monthly-averaged SST anomalies were up to + 1.7 °C, although the temperatures returned to near-seasonal averages after roughly 5 months.

Key words: Hydrography, wind stress, surface temperature, chlorophylls, upwelling.

Caracterización de las condiciones oceanográficas cerca de la Isla Coiba y el Pacífico de Panamá utilizando 20 años de mediciones satelitales de estrés del viento, TSM y clorofila-*a*

RESUMEN. La Isla Coiba y la Zona Especial de Protección Marina asociada representan una reserva marina importante, aunque poco estudiada, a lo largo de la costa del Pacífico de Panamá. Si bien recientemente se han iniciado esfuerzos para establecer programas de monitoreo en la región, ya existe una variedad de mediciones ambientales históricas relacionadas con el mar, derivadas de observaciones satelitales. El objetivo de este artículo fue utilizar conjuntos de datos a largo plazo para variables clave para proporcionar información cualitativa (es decir, oceanografía descriptiva) de las condiciones climatológicas y variabilidad interanual en la región del Pacífico de Panamá. Estos se basan en evaluaciones numéricas, lo que proporciona una base importante para estudios en curso y futuros, particularmente en la región de la Isla Coiba y el Golfo de Chiriquí. En particular, examinamos 20 años (enero de 2003-diciembre de 2022) de estrés eólico, temperatura de la superficie del mar (TSM) y clorofila-*a* (Chl-*a*), que abarcan las regiones neríticas y pelágicas de la costa del Pacífico de Panamá. Durante la estación seca (invierno del norte), el conocido chorro de viento estacional regional de Panamá apareció a lo largo del Golfo de Panamá, lo que provocó una mezcla de la superficie y un enfriamiento de la TSM que finalmente se extendió por la mayor parte de la Bahía de Panamá. Al oeste de la Península de Azuero, la TSM aumentó y el calentamiento de la superficie se extendió más lejos de la costa desde enero hasta abril. La TSM en el Golfo de Chiriquí durante este período fue alrededor de 1 °C más cálida en promedio que al este de la Isla Coiba. En julio y agosto, los gradientes de TSM en alta mar se volvieron en gran medida longitudinales, se produjo un enfriamiento a lo largo de la temporada, y la TSM a ambos lados de la isla Coiba fue casi la misma. La influencia del chorro de Panamá en el Golfo de Panamá también fue evidente en los datos de Chl-*a*, con valores impulsados por las surgencias que alcanzaron su punto máximo en febrero/marzo (hasta 11 mg m⁻³, con un valor climatológico mensual de alrededor de 2 mg m⁻³ durante este período). Durante el resto del año, la concentración de Chl-*a* en esta región promedió alrededor de 0,5-1,0 mg m⁻³. En el Golfo de Chiriquí y la región al este de la Isla Coiba, los promedios climatológicos mensuales fueron aproximadamente 0,3-0,5 mg m⁻³ y 0,4 - 0,6 mg m⁻³, respectivamente. Algo sorprendente es que en los datos satelitales del Golfo de Chiriquí durante mayo de 2007 y junio de 2008 estuvieron presentes valores muy altos de Chl-*a*, alcanzando un máximo de 16 mg m⁻³ y 32 mg m⁻³ en un lugar justo al oeste de la isla Coiba, respectivamente. Aún no está clara la causa de estas aparentes floraciones. Sin embargo, incluso cuando se excluyeron los valores altos de Chl-*a* en el cálculo de los promedios climatológicos en el Golfo de Chiriquí, hay una sugerencia de estacionalidad modesta en los valores de Chl-*a*, con valores ligeramente elevados (~ 0,4 mg m⁻³) que alcanzan su punto máximo alrededor de mayo y octubre. Durante el evento extremo de El Niño de 2015-2016, el promedio mensual de TSM a lo largo de la costa del Pacífico de Panamá fue más cálida que el promedio, con niveles elevados de hasta + 2 °C y con duración de 12 meses en el Golfo de Chiriquí. En el Golfo de Panamá, las anomalías promedio mensuales de la TSM fueron de hasta + 1,7 °C, aunque las temperaturas volvieron a los promedios casi estacionales después de aproximadamente 5 meses.

Palabras clave: Hidrografía, estrés eólico, temperatura superficial, clorofilas, surgencias.

INTRODUCTION

The country of Panama is an isthmus in Central America, located at roughly 7-10° N, 77-83° W, between Costa Rica and Colombia (Figure 1). The largest marine features on the Pacific side of Panama are the Gulf of Chiriquí to the west and the Gulf of Panama to the east; the Azuero Peninsula is a major geographic between the two gulfs. Numerous islands dot the coastal waters: Coiba Island, for example, sits on the southeastern edge of the Gulf of Chiriquí, on the edge of the continental shelf; the Pearl Islands are clustered on the eastern

side of the Gulf of Panama, about 60 km from the shelf edge.

The Pacific Panama coast also represents part of the eastern boundary to the Eastern Tropical Pacific (ETP). Early key research focused on the tuna fisheries and the associated environmental conditions in the ETP (Smayda 1966; Wyrтки 1966). Much of the attention in the past 50 years or so, however, has focused on the importance of the ETP as a component of the Earth's global climate system (the El Niño- Southern Oscillation, ENSO). An excellent set of review papers were published in 2006, spanning overviews of atmospheric conditions (Amador et al. 2006), oceanographic conditions (Fiedler and Talley 2006; Kessler 2006; Willett et al. 2006),

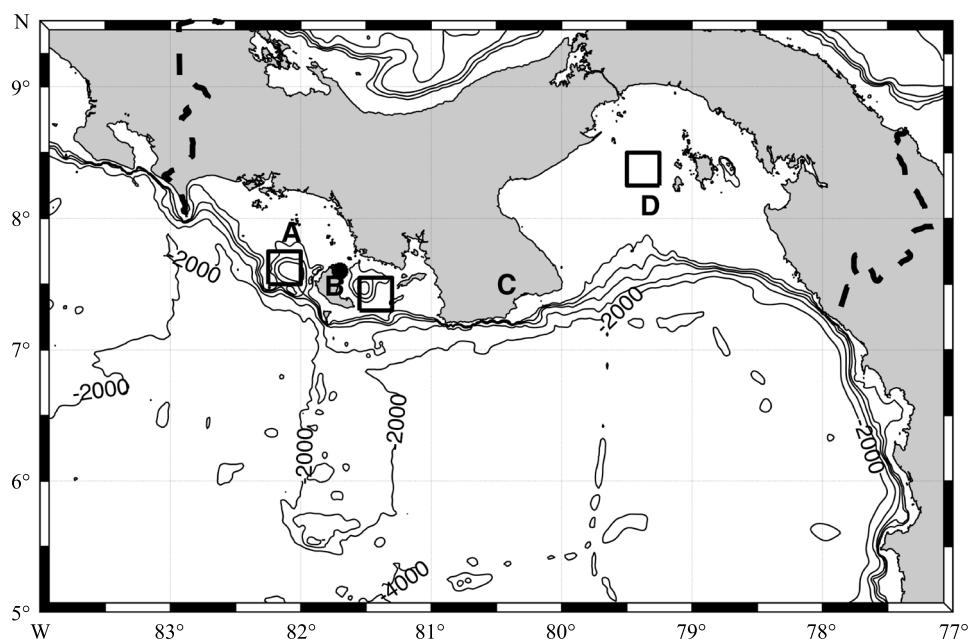


Figure 1. Pacific Panama study region. Key coastal features include the Gulf of Chiriqui (A), Coiba Island (B), the Azuero Peninsula (C), and the Gulf of Panama (D). The Coiba AIP Scientific Station is located on the north side of Coiba Island (black circle). Time series were determined for three geographic subregions (squares): coastal Chiriqui (CC), east of Coiba Island (EC), and the coastal Gulf of Panama (CP). Bathymetric contours are shown for depths of 150, 300, 500, 1,000, 2,000 and 4,000 m; the latter two depths are labeled. Dashed lines represent political boundaries.

biological organisms (Ballance et al. 2006; Fernandez-Álamo and Farber-Lorda 2006; Pennington et al. 2006) and climate variability and change (Mestas-Nunez and Miller 2006; Wang and Fielder 2006). More recent work has been undertaken to understand modes of atmospheric variability in the ETP (Amador et al. 2016a, 2016b; Garcia-Franco et al. 2023). The vast majority of all this research, however, has focused on larger-scale studies in and over the deep ocean.

A more limited set of marine coastal studies in the Pacific Panama region have focused primarily on the Gulf of Panama. Key studies of this region have examined coastal circulation (Corredor-Acosta et al. 2001; Rodriguez-Rubio et al. 2003; Chaigneau et al. 2006; Devis-Morales et al. 2008) and ocean color/chlorophyll concentrations (Rodriguez-Rubio and Stuardo 2002; Corredor-Acosta et al. 2020; Herrera Carmona et al. 2022). A few of these studies do extend to the western edge of

the Pacific Panama coast. The focus on the Gulf of Panama is perhaps not surprising for a number of reasons, including the proximity of the Pacific entrance/exit to the Panama Canal; the Gulf as part of the Panama Bight region, which is adjacent to part of the Colombian coastline; and the annual wind-driven upwelling in the Gulf and Bight that plays an important role in the local ecosystem.

On the other hand, there has been a growing need for improved monitoring and understanding of the marine environment in the Gulf of Chiriqui region, particularly in the Coiba Island region. In 1992, the government of Panama created Coiba National Park, a marine reserve including Coiba Island. In 2004, the government refined and expanded the region as the Coiba National Park and its Special Zone of Marine Protection, spanning a total of area of 4,300 km². It was subsequently identified as a World Heritage Site by UNESCO. Coiba National Park is considered a biological sanctuary and

hotspot for species and ecosystem diversity where elevated functional and demographic connectivity with other ETP islands have been demonstrated for megafauna, fishes, corals, and zooplankton (Alvarado et al. 2012; Guzmán et al. 2021; Brugnoli Olivera et al. 2023). Despite its conservation status and reduced visitation, potential threats to biodiversity have been identified in the area, including the introduction of invasive species, micro and macro plastic pollution, illegal fisheries, and climate change impacts such as coral reef bleaching (Podesta and Glynn 1997; Colley et al. 2006; Maté et al. 2009). The region also lies within the Eastern Tropical Pacific Marine Corridor (CMAR), a multi-national initiative for conservation, protection and sustainable use of marine resources that also includes the Galapagos Islands (Ecuador), Malpelo and Gorgona Islands (Colombia) and Coco Island (Costa Rica) (Enright et al. 2021).

To this point, there has been relatively little research in the Gulf of Chiriqui/Coiba region. Most of what has been published has focused on coral reef studies (D’Croz and Robertson 1997; Camilli et al. 2007, 2008; D’Croz and O’Dea 2007) and temperature effects on coral bleaching (Podesta and Glynn 1997; Colley et al. 2006). A notable exception to this is D’Croz and O’Dea (2007), who conducted four cruises in the region, spanning different times of year, and assessed the extent and impact of upwelling in the Gulf of Panama and the Gulf of Chiriqui. The establishment of Coiba AIP (‘Asociación de interés público’ in Spanish) and the recent creation of a scientific research station on Coiba Island represent significant steps towards increasing the capacity for *in situ* environmental assessment and monitoring in the region (Cardona et al. 2021; Guzmán et al. 2021; Brugnoli Olivera et al. 2023). However, there is a wealth of historical, publicly-available, nearly continuous (in time and space) satellite-based data products that can provide information on climatological and anomalous conditions in the marine environment.

Some satellite data have been used in the past to characterize marine environmental conditions and

relationship in the ETP in general (Amador et al. 2016a, 2016b), with some emphasizing conditions in the Panama Bight (Rodríguez-Rubio and Stuardo 2002; Corredor-Acosta et al. 2020; Carmona et al. 2022). The present study is the first of its kind to focus on characterizing seasonal climatologies and interannual variability of satellite-derived sea surface temperature (SST) and chlorophyll-*a* (Chl-*a*) concentrations over the Pacific Panama continental shelf, including sites in the vicinity of Coiba National Park and its Special Zone of Marine Protection. We also assessed the apparent impact of the 2015-2016 El Niño, considered to be one of the three strongest and long-lived such events since 1950 (Santoso et al. 2017; Hu and Fedorov 2019) but little discussed thus far in the scientific literature in terms of the coastal Pacific Panama region.

MATERIALS AND METHODS

For this study, we examined 20 years (January 2003–December 2022) of wind stress (estimated for 10 m height; 25 km resolution), SST (4 km resolution), and Chl-*a* (4 km resolution). Data were accessed through the NASA (U.S. National Aeronautics and Space Administration) Giovanni website/interface (see Acker and Leptoukh 2007). Sea surface temperature and Chl-*a* data used here were derived from MODIS Aqua data (Level 3). Climatological averages for each month were generated from monthly-averaged SST data (NASA OBPG 2019a) and from 8 d-averaged Chl-*a* data (NASA OBPG 2022), respectively. Monthly wind stress climatologies were calculated from the MERRA-2 (Modern-Era Retrospective analysis for Research and Applications version 2) data set of time-averaged, two-dimensional monthly mean values, assessed at 10 m height (GMAO 2015).

For SST and Chl-*a* time series, we used the 8-d composite data sets (NASA OBPG 2019b; 2022). We averaged these data over 4×4 pixels (roughly 300 km^2) in three regions (see Figure 1): a location

in the coastal Gulf of Chiriqui (CC) region, near the edge of the continental shelf and just west of Coiba Island; a region east of Coiba Island (EC); and a site near the middle of the Gulf of Panama (CP). Data were downloaded and then subsequently analyzed and imaged using Matlab (The Mathworks Inc. 2022) and M_Map (Pawlowicz 2021). A Pearson correlation coefficient, ρ , was determined for SST and \log_{10} (Chl-*a*) at each of the three sites. We also examined some of the fundamental optical measurements that are used to calculate Chl-*a* estimates. The algorithm used to estimate surface ocean Chl-*a* concentrations is described in Hu et al. (2019) and O'Reilly and Werdell (2019). It is noted that for high Chl-*a* concentrations ($> 0.35 \text{ mg m}^{-3}$), the algorithm uses a ratio of the (logarithm of the) relative reflectance, R_{rs} , from the ocean surface at blue and green wavelengths. For MODIS Aqua chlorophyll calculations, the green wavelength band was centered at 547 nm, while there were two dataset options for the blue wavelength: 443 nm and 488 nm (O'Reilly and Werdell 2019). The algorithm used whichever ratio yields the highest value: ($R_{rs}(443 \text{ nm})/R_{rs}(547 \text{ nm})$) or ($R_{rs}(488 \text{ nm})/R_{rs}(547 \text{ nm})$). In the present study, for illustrative purposes, time series of $R_{rs}(488 \text{ nm})$ and $R_{rs}(547 \text{ nm})$ were examined.

Daily precipitation rate data were examined for a region over the coastal Gulf of Chiriqui and southwestern Panama ($8.125\text{-}8.375^\circ \text{ N}$, $81.625\text{-}81.875^\circ \text{ W}$), using the Global Precipitation Measurement (GPM) Integrated Multi-satellitE Retrievals for GPM (IMERG) dataset (Huffman et al. 2023). Data were smoothed with an 8-day running average.

RESULTS

A strong southward wind stress was present over the Gulf of Panama from January through March (in fact it actually began in December), concomitant with SST cooling within and south of

the Gulf, with average SST dropping to as low as $\sim 25^\circ \text{ C}$ (Figure 2). South of the Azuero Peninsula and further west, winds were generally southward, although their strength tapered off to the west. The SST in the Gulf of Chiriqui warms up from January through April from about 29° C to 30° C during the dry season; the warmed region also extends offshore across this period. A strong, largely zonal SST gradient existed between the Gulf of Chiriqui and the Gulf of Panama of up to 5° C across roughly 200 km; the SST on the west side of Coiba Island was on average about 1° C warmer than on the eastern side.

As March gave way to boreal spring, winds first slackened and then blew roughly to the east-northeast. The strong zonal SST gradient was wiped away by May, replaced by a largely meridional gradient, with coastal SST in the Gulf of Chiriqui and Gulf of Panama ranging around $29\text{-}30^\circ \text{ C}$ in August. Further offshore in oceanic waters (e.g. south of about 6° N) there was a general cooling trend in SST from June through November, dropping from about 28° C to 27° C . Warmer SSTs ($\sim 29\text{-}30^\circ \text{ C}$) were relegated to the shelf regions from June through September. By October, the SST over the outer region of the Gulf of Chiriqui and off the Azuero Peninsula dropped to near-oceanic levels, although warmer SST values ($\sim 29^\circ \text{ C}$) were present in the Gulf of Panama into November. By December, warming of the SST on the western side of Pacific Panama had begun again, while some southward wind flow occurred over the Gulf of Panama and the SST remained fairly cool ($\sim 28^\circ \text{ C}$).

The strong seasonal cycle in SST was clearly seen in CP and CC (Figure 3). The extent of SST cooling and its duration during the January-March upwelling period varied extensively, with 2019 representing a prolonged period (almost 3 months) of significant SST cooling ($22\text{-}24^\circ \text{ C}$). On the other hand, there was a similar degree of cooling in 2012, but it lasted about half as long. There was little sense of a seasonal signal, visually, in the EC time series plot. The annual average SST at CC, EC and CP was 29.3° C , 29.0° C and 28.0° C ,

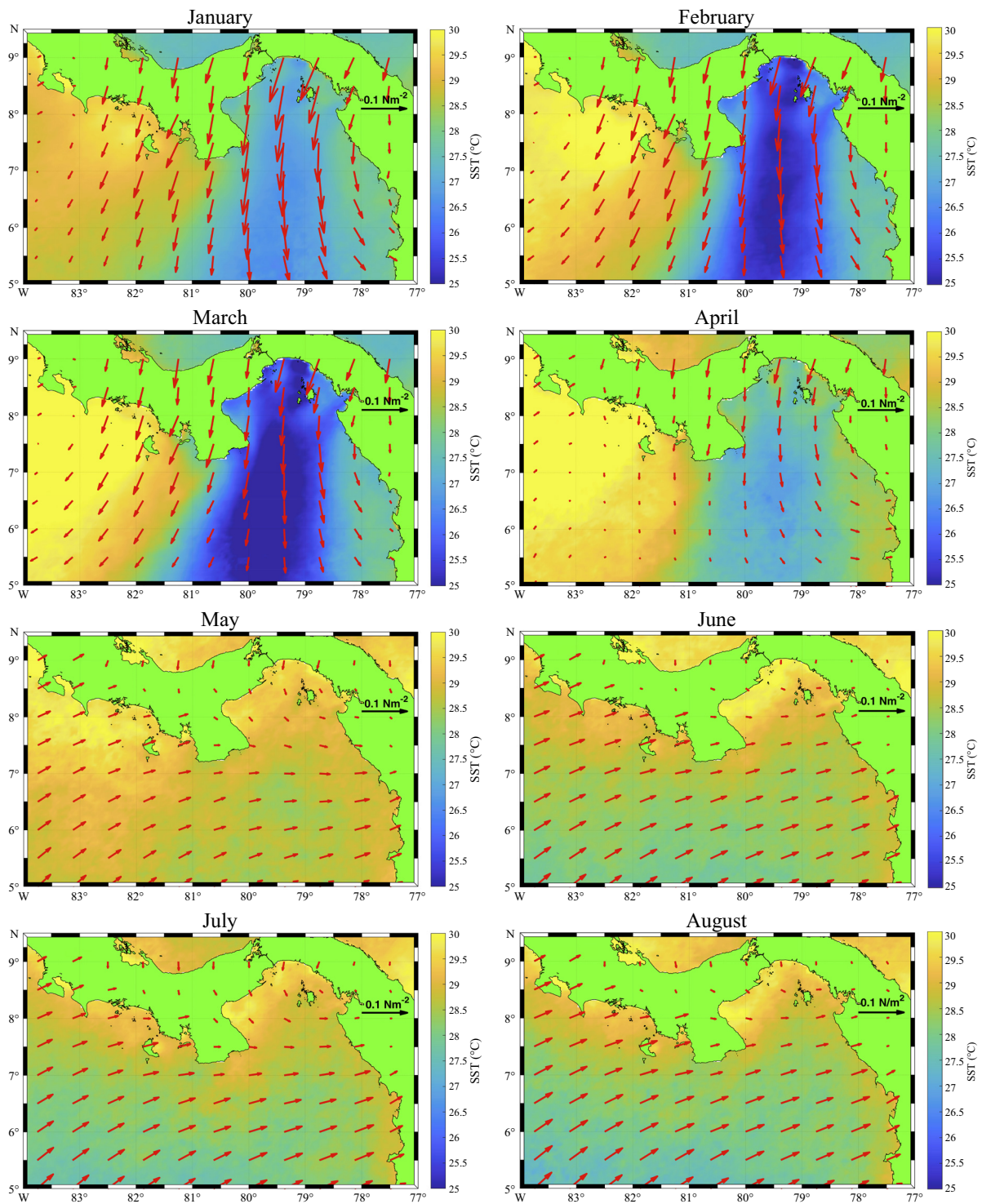


Figure 2. Monthly climatology maps of mean wind stress and SST for January through December, derived from the 20-year data sets.

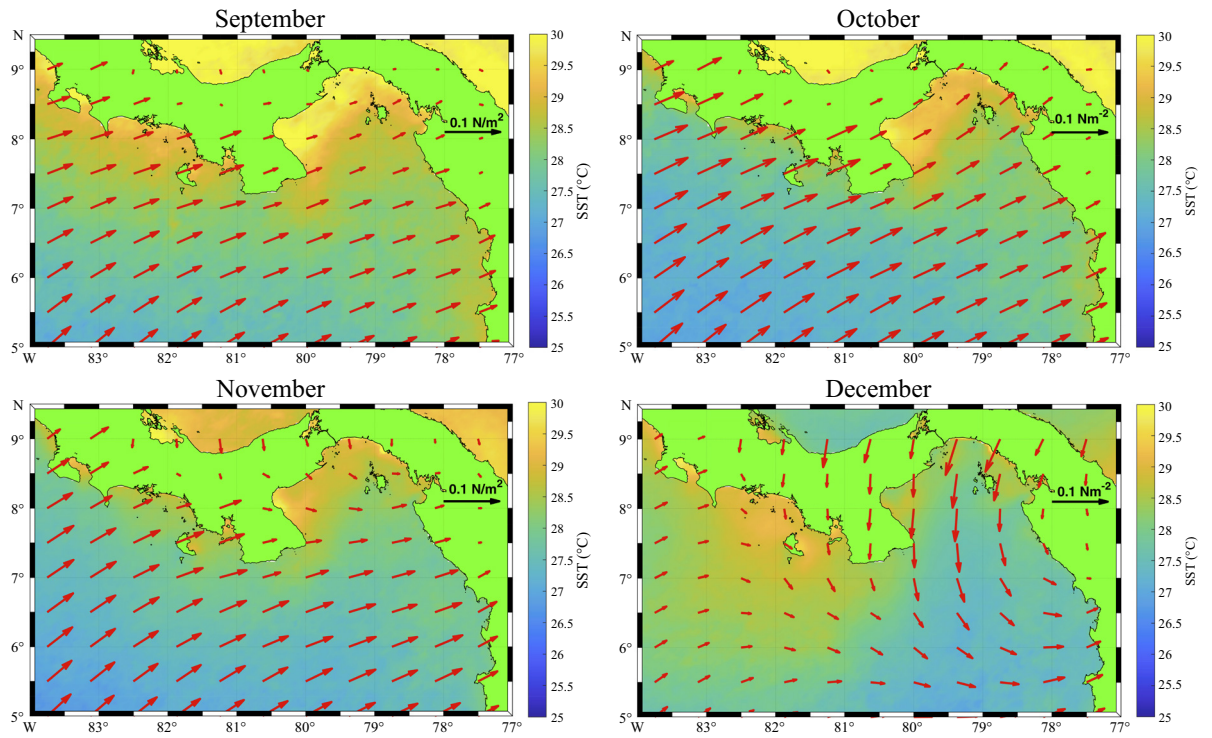


Figure 2. Continued.

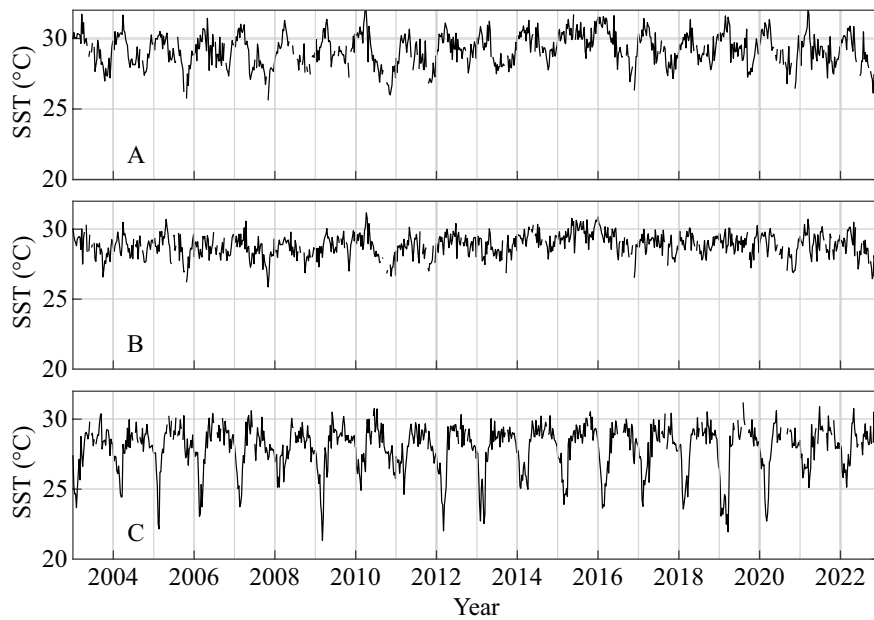


Figure 3. Sea surface temperature SST time series from January 2003 through December 2022 at Gulf of Chiriqui (CC) (A), Coiba Island (EC) (B), and Gulf of Panama (CP) (C), based on 8-d averages.

respectively. The greatest range in SST occurred at CP (21.3-31.2 °C) and the smallest occurred at EC (27.1-29.0 °C). At CC, the range was 25.5-32.2 °C.

Broadly speaking, Chl-*a* values on the order of 0.5 mg m⁻³ or less were observed across the oceanic and most of the coastal regions most of the time (Figure 4). In some regions very near the coastline (e.g. Gulf of Montijo, between Coiba Island and the Azuero Peninsula; along the northern shoreline in the Gulf of Panama), monthly estimates of Chl-*a* were significantly enhanced (~ 5 mg m⁻³) over much of the year.

Strong winds associated with the Panama jet in January-March were associated with a broad band of elevated Chl-*a* in the Gulf of Panama and extending further south, averaging 2-4 mg m⁻³ over the month of February (Figure 4). By April, the feature has largely disappeared/dissipated and for the rest of the year the Chl-values were relatively low. Somewhat surprisingly, there appears to be a slight elevation in Chl-*a* estimates in the Gulf of Chiriqui region in May and June, up to around 2 mg m⁻³.

Some gaps can be seen in the Chl-*a* time series data derived from the 8-d composite images and averaged over the regions CC, EC and CP (Figure 5). Persistent cloud cover, for example, can impede the retrieval of Chl-*a* estimates from satellite data. The annual cycle in Chl-*a* at CP, driven by the Panama jet winds, was very clear (Figure 5, bottom panel); values ranged from 0.2 to 11.0 mg m⁻³, with peak values typically occurring in February and March. No particular seasonal signal was evident at EC; the range of Chl-*a* values was 0.1-2.2 mg m⁻³. Similarly, there was not an obvious annual cycle at CC. However, there were five of the 8-day Chl-*a* values at CC that were notably higher than the rest, specifically: May 1, 2007 (16.0 mg m⁻³); May 9, 2007 (16.0 mg m⁻³); May 24, 2008 (9.6 mg m⁻³); June 9, 2008 (31.9 mg m⁻³); and June 17, 2008 (9.1 mg m⁻³). The remainder of the Chl-*a* data at CC ranged between 0.1 and 2.0 mg m⁻³. At EC, there was little sense of seasonal variability. The Chl-*a* values here ranged between 0.2 and 3.2 mg m⁻³.

To provide more insight regarding the two periods of substantially enhanced Chl-*a* estimates in the Gulf of Chiriqui, monthly averaged maps Chl-*a* maps for the Pacific Panama region for April-June 2007 and for May-July 2008 were generated (Figure 6). In April 2007, there was some sense of elevated Chl-*a* values in the Gulf of Chiriqui, although it was confined to the nearshore region of the shelf. In May, high values (> 3 mg m⁻³) in the gulf extended out to the shelf edge and beyond. At the east of Coiba Island and in the Gulf of Panama, no such enhancement was present. By June, elevated levels in the Gulf of Chiriqui (N. B. cloud cover likely dominated the nearshore region during this month). For the 2008 event, there appeared to be enhanced Chl-*a* levels across the inner shelf of the Gulf of Chiriqui and along the western edge of Coiba Island already present in May. By June, the enhanced levels extended all the way across the shelf and out about 100 km offshore. By July, high values have largely dissipated except for close to the shoreline.

Pearson correlation coefficients (ρ) for CC, EC and CP, and for the aggregated data were -0.27, -0.15, -0.68, and -0.58, respectively (Figure 7). If we remove the five anomalously high Chl-*a* data points at CC previously identified, then the correlation coefficients for CC and for the aggregated data become -0.34 and -0.61, respectively.

Time series of $R_{rs}(488 \text{ nm})$ and $R_{rs}(547 \text{ nm})$ for an abbreviated time period (2006-2010) at CC, EC and CP showed that large Chl-*a* values at CC in 2007 and 2008 were clearly associated with a significant drop in reflectance at 488 nm (Figure 8). A similar result was observed at 443 nm (not shown). At CP, seasonal increases in Chl-*a* in February and March of each year were also associated with reduced values at 488 nm. At EC, the ratio of the reflectance at 488 nm and at 547 nm remained consistent through the year, coinciding with the observation of very little variation in Chl-*a* estimates at this location.

To try to assess what may have been responsible for high satellite-derived Chl-*a* values at CC

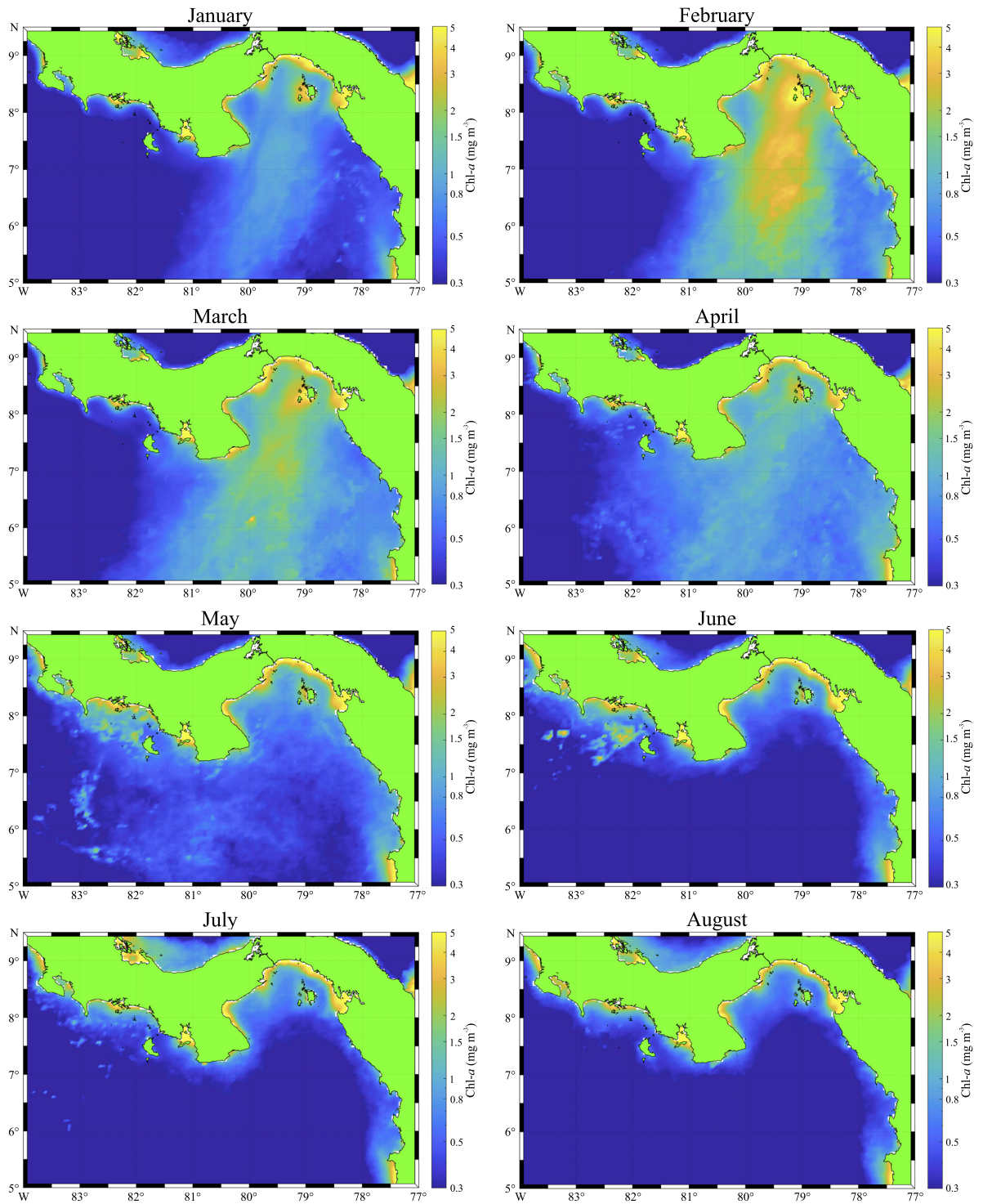


Figure 4. Monthly climatology maps of Chl-a concentration for January through December, derived from the 20-year data sets.

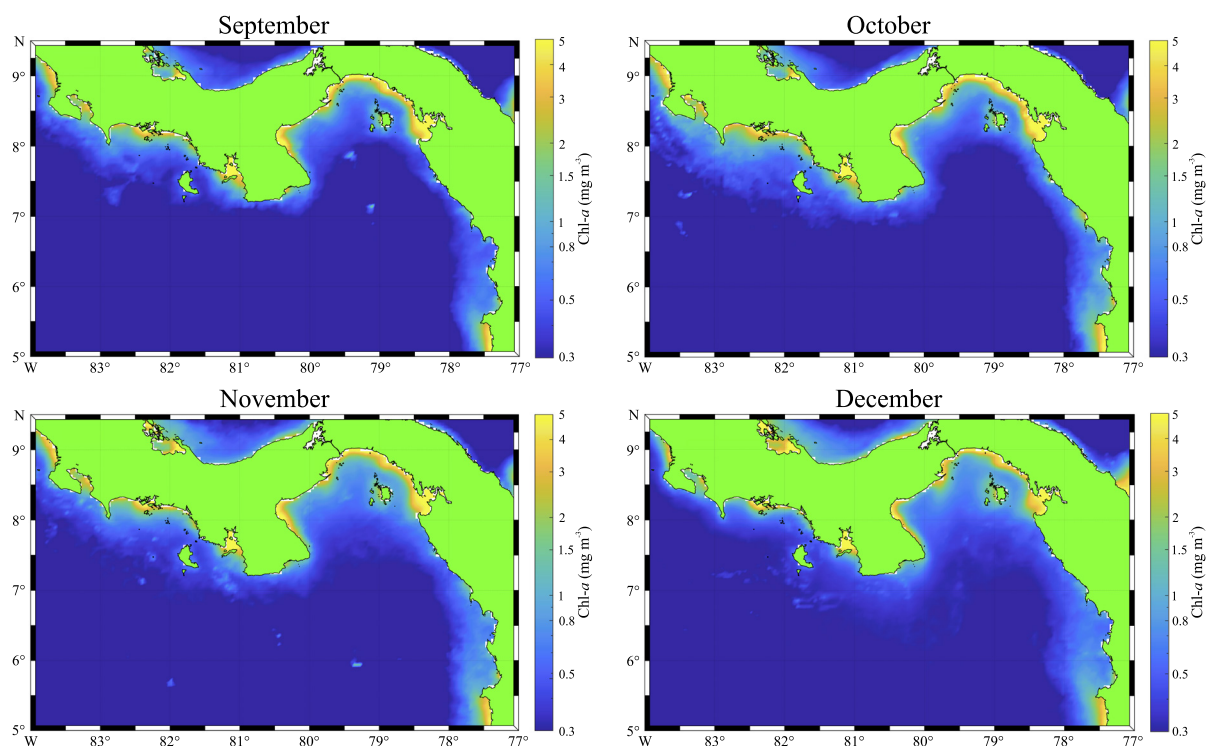
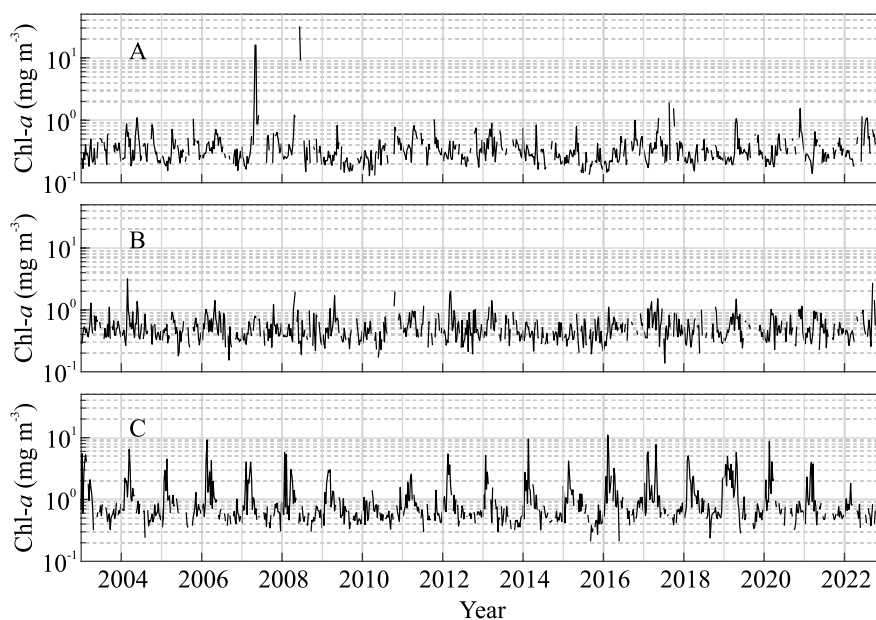


Figure 4. Continued.

Figure 5. Chl-*a* time series from January 2003 through December 2022 at Gulf of Chiriqui (CC) (A), Coiba Island (EC) (B), and Gulf of Panama (CP) (C), based on 8-d averages. Data gaps are typically due to atmospheric effects (e.g. extended cloud cover).

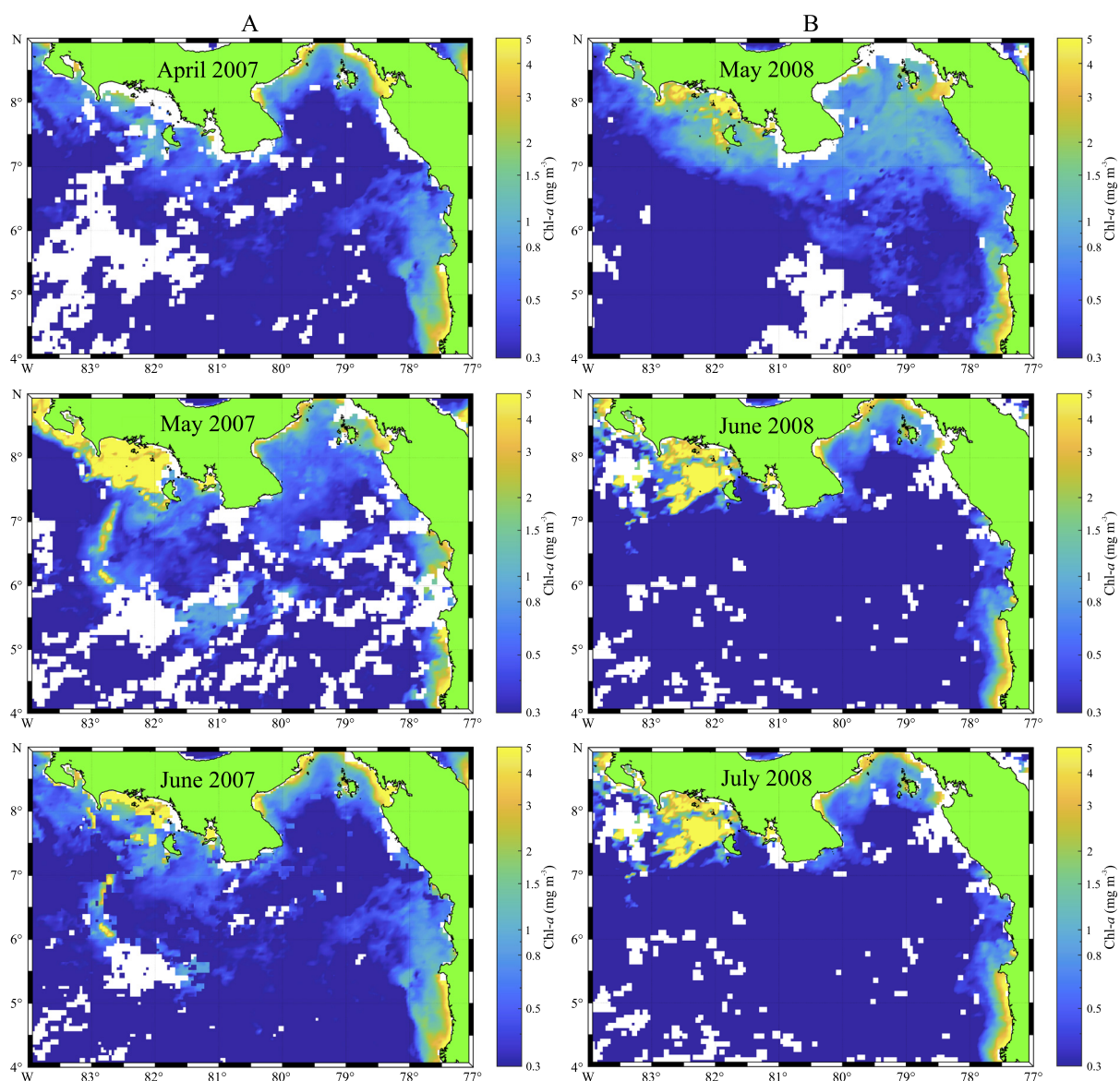


Figure 6. Monthly mean Chl-*a* concentrations across two events where high values were observed in the Gulf of Chiriqui: May 2007 and June 2008. April–June 2007 (A) and May–July 2008 (B).

in 2007 and 2008, we considered both locally wind-driven upwelling and the potential influence of significant runoff to the Gulf of Chiriqui (e.g. large inputs of terrestrially-derived nutrients; potential contamination of Chl-*a* estimates due to large inputs of terrestrially-derived gelbstoff and/or colored dissolved organic matter, CDOM) (Har-

vey et al. 2015; Lavigne et al. 2021). In terms of locally wind-driven upwelling, the monthly mean wind stress near CC was relatively low ($4.7 \times 10^{-2} \text{ Nm}^{-2}$, to the north-northeast) though higher than the mean value for May ($2.7 \times 10^{-2} \text{ Nm}^{-2}$; to the north-northeast). The mean wind stress for June 2008 at CC ($3.0 \times 10^{-2} \text{ Nm}^{-2}$; to the north-north-

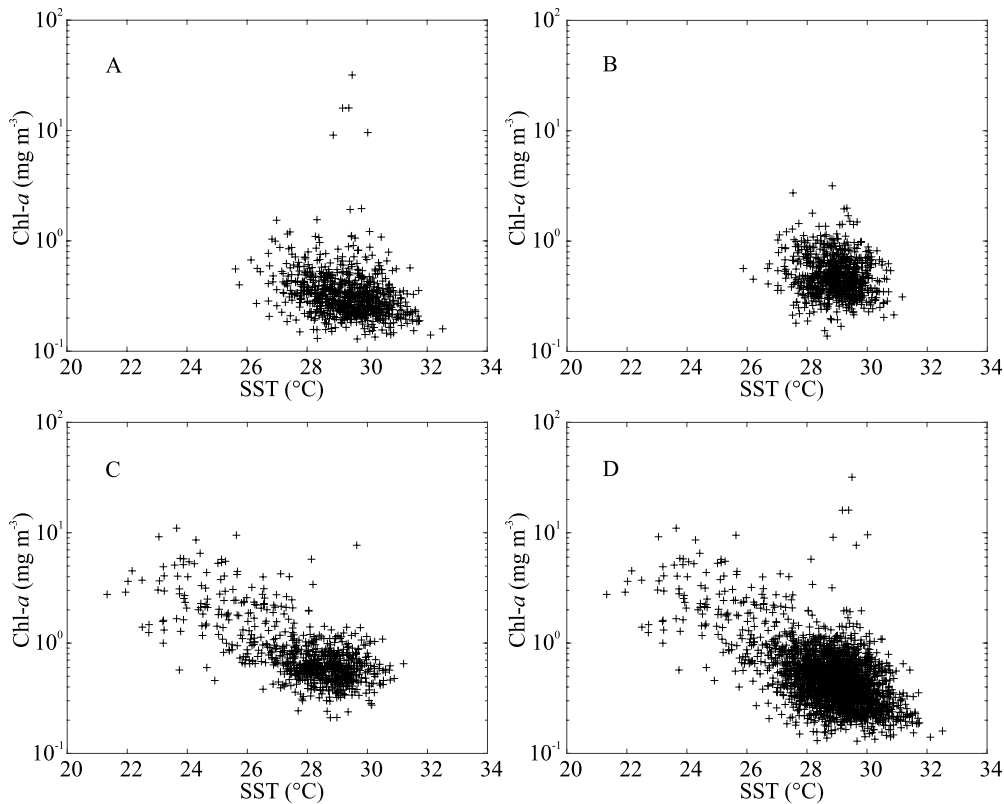


Figure 7. Scatterplots of Chl-*a* v. SST, based on 8-day averages for Gulf of Chiriqui (CC) (A), Coiba Island (EC) (B), Gulf of Panama (CP) (C), and all three locations (aggregated data) (D). Pearson correlation coefficients for the four data sets were $\rho = -0.27, -0.15, -0.68$ and -0.58 , respectively. If the 5 anomalously high Chl-*a* values at CC are ignored, then $\rho = -0.34$ and -0.61 for (a) and (d), respectively.

east) was similar to the climatological mean for June ($3.5 \times 10^{-2} \text{ Nm}^{-2}$, to the north-northeast).

Chlorophyll-*a* estimates at CC during 2006 peaked at 0.7 mg m^{-3} around May 1 of that year (Figure 9). A modest rainstorm occurred around April 27, with a peak average rainfall rate of about 1.5 cm d^{-1} . The next significant storm arrived around May 19, with a peak (8-day running average) rainfall rate of 2.3 cm d^{-1} . There was little suggestion of an increase of Chl-*a* during this latter period. For the 2007 event, Chl-*a* began to rise around day April 23 (2.0 mg m^{-3}), peaking around 16 mg m^{-3} by May 1 through May 9. Averaged rainfall rates in the Gulf of Chiriqui region were roughly 0.7 cm d^{-1} around April 14. Another slightly strong rainstorm arrived centered around April

29 and averaged around 1 cm d^{-1} . A third storm arrived between roughly May 11 and May 21 with average rainfall rates peaking around 2 cm d^{-1} , although this was after the Chl-*a* event.

For the 2008 high Chl-*a* event at CC, there was a significant gap in Chl-*a* estimates between April 30 (when Chl-*a* estimates were slightly elevated, around 1 mg m^{-3}) and June 9 (when the Chl-*a* peaked at 32 mg m^{-3}). There were two substantial rainfall events, centered around May 11 and May 24 (with average precipitation rates of up to 2 cm d^{-1} and 3 cm d^{-1} , respectively). For 2009, there was a major, extended period of rainfall lasting about 2 weeks, peaking around May 23 and averaging as much as 5 cm d^{-1} across an 8-day period. Chlorophyll-*a* peaked at around 0.8 mg m^{-3} by May 17.

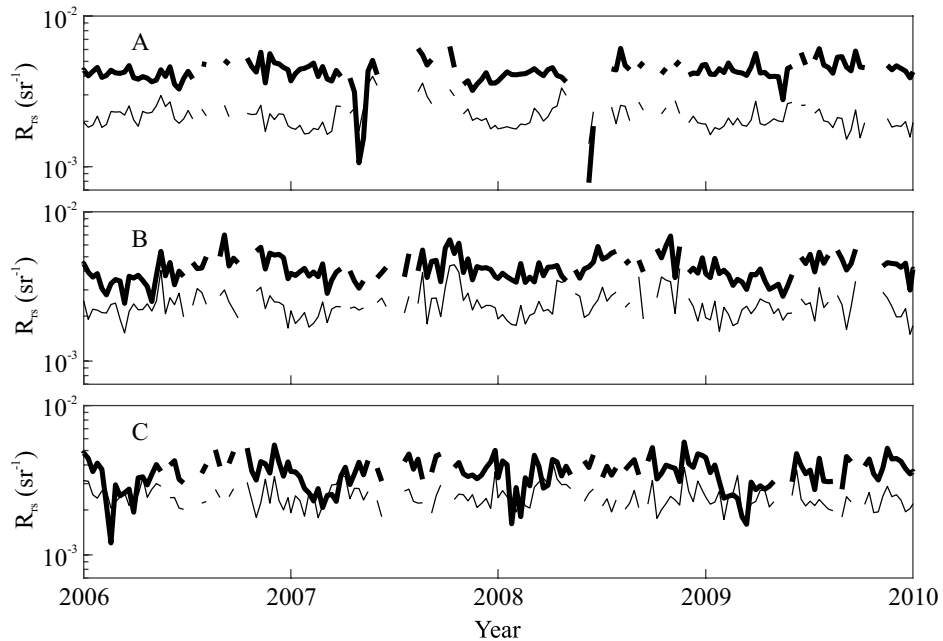


Figure 8. Eight-day average relative reflectance, R_{rs} , at 488 nm (thick line) and 547 nm (thin line) from 2006–2010 at: Gulf of Chiriqui (CC) (A), Coiba Island (EC) (B), and Gulf of Panama (CP) (C).

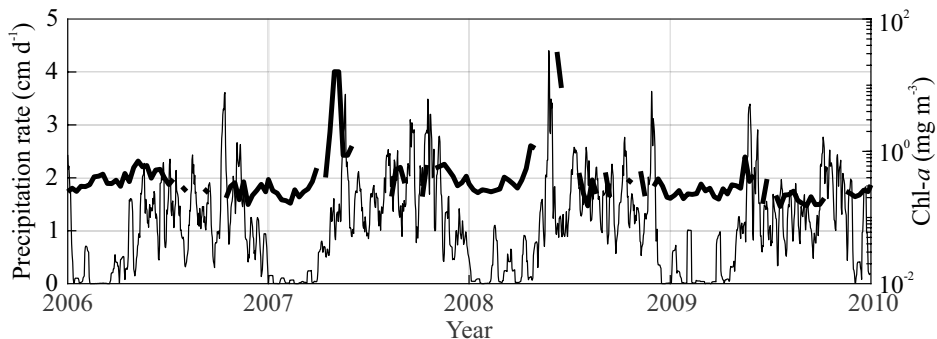


Figure 9. Eight-day averaged Chl-*a* estimates at CC (thick line) and daily precipitation rate (thin line) over a region of the coastal Gulf of Chiriqui and southwestern Panama (8.125–8.375° N, 81.625–81.875° W) for the period 2006–2010. The daily precipitation rates were smoothed with an 8-day running average to facilitate comparison with the Chl-*a* data.

In terms of probability distributions, Chl-*a* values were closer to a lognormal distribution, while SST data were more normally distributed (not shown). In order to estimate monthly climatology values for CC, EC and CP, we have binned and averaged SST and $\log_{10}(\text{Chl-}a)$ time series data from Figure 3 and 5, respectively, by month. In addition, given that Chl-*a* data from May 2007 and June

2008 were so anomalously high and their cause remains poorly understood, we have excluded the previously identified five 8-day average data points from this analysis (Figure 10). The seasonal cooling of SST and increase of Chl-*a* in coastal Panama, associated with the Panama jet, was clearly seen. In February, the monthly climatological mean SST and mean Chl-*a* at CP were 25.3 °C and 1.8 mg m⁻³,

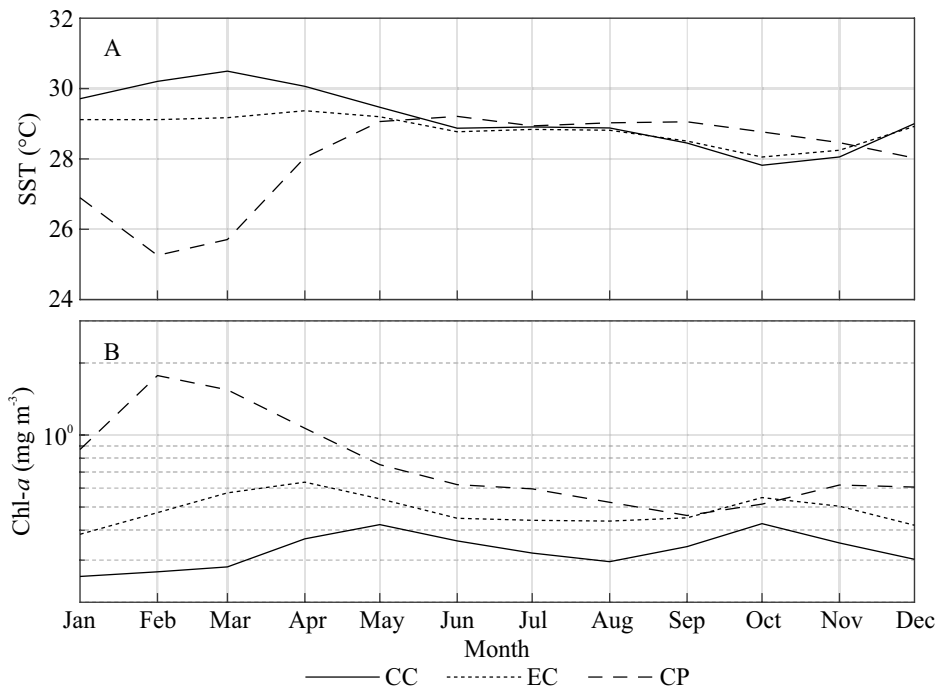


Figure 10. A) Mean monthly SST climatology at Gulf of Chiriqui (CC), Coiba Island (EC), and Gulf of Panama (CP) from SST time series (see Figure 3). B) Monthly Chl-*a* climatology at CC, EC, and CP, calculated from Chl-*a* time series (see Figure 5) and based on mean [$\log_{10}(\text{Chl-}a)$].

respectively. As noted previously, from January through April, the mean SST on the western side of Coiba Island was roughly 1 °C warmer than the eastern side (~ 30 °C versus ~ 29 °C), although the two track each other through the rest of the year. Climatological monthly averages of Chl-*a* at EC were slightly higher at EC than at CC by about 0.1 mg m⁻³ through most of the year.

In order to assess the impact of the very large 2015-2016 El Niño event along the Pacific Panama coast, we determined the monthly mean SST anomalies at CC, EC and CP and CC for January 2015 through December 2016 (Figure 11). In the Gulf of Chiriqui, the monthly-averaged SST anomaly was elevated for 12 months (April 2015 through March 2016), averaging + 1.5 °C during this period and peaking at + 1.9 °C around December 2015-January 2016 (Figure 11). At EC, the monthly-averaged SST anomaly was similarly elevated for 10 months (May 2015-February 2016), peaking

around + 1.6 °C in December 2015. In contrast, the monthly averaged SST at CP was elevated for roughly 5 months (September 2015-January 2016), peaking at about + 1.6 °C and averaging + 0.9 °C.

DISCUSSION

As has been discussed elsewhere, the Panama jet largely dominates the wind patterns in January-March, generating some deepening of the mixed layer in the Gulf of Panama and driving surface waters offshore (D’Croz et al. 2001; Rodriguez-Rubio et al. 2003; Corredor-Acosta et al. 2020). Both effects lead to upwelling conditions, which drives increased productivity in and south of the Gulf of Panama for 2-3 months.

The wind stress across the Gulf of Chiriqui is lower during January-March than that over the Gulf

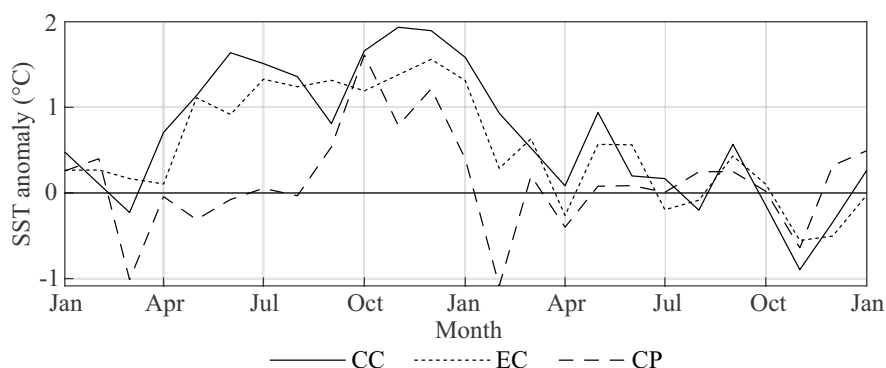


Figure 11. Monthly-averaged anomaly time series of SST at ulf of Chiriqui (CC), Coiba Island (EC), and Gulf of Panama (CP) during the 2015-2016 El Niño event.

of Panama (although the direction of winds across the entire region is largely southward). Wind mixing is therefore also expected to be lower and there is little evidence of upwelling. Furthermore, there is no evidence of seasonal upwelling in these regions. During the dry season, the SST actually increases in the Gulf of Chiriqui and warmer surface waters extend further away from the coast. This appears to be largely a consequence of the very high incoming shortwave radiative fluxes in the region during this time (see Amador et al. 2006). Interestingly, the SST in the Gulf of Chiriqui and west of Coiba Island is about 1 °C warmer than east of Coiba Island during this time. The region between Coiba Island and the eastern edge of the Azuero Peninsula appears to represent a transition zone between the two regimes. This thermal gradient may represent a seasonal barrier to exchanges between the two gulf regions.

April and May represent transition months between dry and wet seasons, with the Panama jet disappearing and the ITCZ shifting north (Amador et al. 2006), establishing wind patterns that blow to the east and east-northeast. During this time, the SST increases in the Gulf of Panama. As July proceeds into August, the ITCZ is roughly over Costa Rica and Panama. By June and July, SST gradients are quite meridional in general (and roughly parallel to the Panama coastline; see also Corredor-Acosta et al. 2020). Some net cooling of the SST occurs across the region. The SST in

the Gulf of Chiriqui and the eastern side of Coiba Island are nearly uniform for most of this period.

As the ITCZ shifts further southward, mean wind patterns remain fairly similar through until December. Net cooling of the SST continues across much of the domain through until roughly November, although the net impact in the coastal regions is lower (~ -0.5 °C from July to October at CC and EC; little discernible change at CP) than in the pelagic regions (~ -1 °C from July to October). This is presumably at least partly due to lower wind stress over the continental shelf over Pacific Panama. By December, preliminary signs of a return to the dry season are present, as SST increases slightly at CC and EC.

The El Niño event of 2015-2016 was the largest event in the past 25 years. Effects of the event were observed in SST anomalies along the Panama coast, although the impact appeared greater in the Gulf of Chiriqui and east of Coiba Island, both in terms of duration and increase in SST (e.g. averaging +1.3 °C across 12 months at CC) than in the Gulf of Panama (averaging +0.9 °C across 5 months at CP). This would seem to be at least partly a consequence of the fact that the Gulf of Chiriqui is more exposed to the open ocean, while the Gulf of Panama is more sheltered. Such events might therefore be expected to have a more dramatic impact on the marine environment (e.g. coral reefs) in the Gulf of Chiriqui than in the Gulf of Panama.

In general, SST at EC changes very little through the year, compared to CC and CP. Like CC, EC is not strongly influenced by the Panama jet; furthermore, the region is fairly confined by Coiba Island to the west and the Azuero Peninsula to the east. It is certainly reasonable to assume that longitudinal advection and diffusion are fairly limited here, which may help to constrain SST variations.

How accurate are satellite-derived Chl-*a* estimates? Certainly, concerns exist because of potential interference due to the presence of suspended particulate matter (SPM) and/or colored dissolved organic matter (CDOM) (Harvey et al. 2015; Lavigne et al. 2021). When *in situ* data are available for coastal waters, it is possible to modify the algorithms used for calculating Chl-*a* (Tilstone et al. 2013; Jiang et al. 2017). In regions such as the coastal ETP, however, very little *in situ* observations have been available to this point. Pennington et al. (2006) compared Chl-*a* measurements in the ETP based on available ship-collected Chl-*a* measurements derived from various sources and on SeaWiFS (i.e. the predecessor to the MODIS Aqua satellite instrument) estimates from 1980-2005. They looked at both monthly averages and an overall average for the period. In the Gulf of Panama region, the SeaWiFS values overestimated the *in situ* observations through the year by a factor of 2-3 (see figure 8 D from Pennington et al. 2006), although the seasonal trends were quite consistent across the two data sets. Camilli et al. (2008) compared SeaWiFS data with *in situ* data from a tow-fish on a much smaller time and space scale, in a region between Coiba Island and the mainland during a roughly two week period in February 2007. They found generally reasonable agreement (averaging around 0.20 to 0.25 mg m⁻³ during this period), although the *in situ* measurements were made at a much finer spatial and temporal resolution than the satellite data (9 km² resolution) and showed much more variability.

The only shipboard observations of Chl-*a* in the Pacific Panama region during the 2003-2022 period, of which we are aware, were presented in

D’Croze and O’Dea (2007), who made shipboard measurements of Chl-*a* in the Gulf of Chiriqui and the Gulf of Panama during December 14-20, 2004. Those observations can be compared directly against the satellite-derived observations. In addition, D’Croze and O’Dea (2007) made observations during three additional cruises that occurred before 2003. These were compared against monthly climatological means derived for the 2003-2022 period (Table 1). In the Gulf of Chiriqui, the shipboard and satellite-derived values are generally low and compare favorably, typically within a factor of two. In the Gulf of Panama, satellite-derived values are more often higher than the *in situ* observations by a factor of roughly two, overall. Within the very limited datasets available, we suggest that satellite-based and shipboard measurements of Chl-*a* are generally comparable or within a factor of two, with satellite values more likely to be higher than the *in situ* observations.

Overall, the well-known seasonal variation in upwelling and primary productivity in the Gulf of Panama region is well-represented in the climatology data. There appears to be a fairly strong inverse correlation between SST and log₁₀ (Chl-*a*) ($\rho = -0.68$). This is not surprising, given the well-known connection between the annual arrival of the Panama wind jet and the subsequent coastal upwelling in the Gulf of Panama. In the Gulf of Chiriqui region, west of Coiba Island, there appears to be only a weak inverse correlation ($\rho = -0.27$) between SST and log₁₀ (Chl-*a*). If the high Chl-*a* values from May 2007 and June 2008 are excluded, the correlation only increases to $\rho = -0.34$. Unlike the Gulf of Panama, the Gulf of Chiriqui does not have the annual wind-driven upwelling driving SST cooling, upwelling of nutrients and increases in primary productivity. At EC, the correlation is even weaker ($\rho = -0.15$), perhaps partly due to a smaller range of SST and Chl-*a* values than either CC or CP.

Recently, Herrera Carmona et al. (2022) identified 11 different dynamic biogeographic regions (DBGs) and assessed monthly climatologies of SST and Chl-*a* from each. This provides an oppor-

Table 1. Comparison of average *in situ* measurements of Chl-*a* (D’Croze and O’Dea 2007), corresponding to the Gulf of Chiriqui (CC) and the Gulf of Panama (CP), and 8-day averaged, satellite-derived Chl-*a* estimates, corresponding to CC and CP. The satellite-derived data (from this paper) are provided in parentheses. The shipboard data represent the median observed Chl-*a* values observed in the upper 20 m of the water column. For the December 2004 data, we use satellite-derived data corresponding to December 18, 2004. For the other three shipboard sampling periods, we use the monthly climatological values for comparisons (see Figure 10). Measurements are in mg m^{-3} .

	February 2000	June 2001	August 1999	December 2004
Gulf of Chiriqui (CC)	0.29 (0.26)	0.16 (0.36)	0.34 (0.30)	0.17 (0.21)
Gulf of Panama (CP)	1.44 (1.77)	0.83 (0.62)	0.27 (0.52)	0.24 (0.52)

tunity to compare the results described here to their analyses. One DBGR, identified as ‘Panama Gulf (R7)’, covers much of the Gulf of Panama, out to about 75 km offshore, and includes CP roughly in the middle of the domain. Another region, labelled ‘PB Transition (R6)’ (with PB referring to the Panama Bight) includes the region out to about 125 km south of R7, as well as a region offshore of the Columbia continental shelf (out to about 75 km from the coast), the region between Coiba Island and the Azuero Peninsula, and the inner half (out to about 30 km offshore) of the Gulf of Chiriqui (EC lies within this region). The region identified as ‘Panama Bight East (R4)’ spans a large swath south of R6, but also includes the outer shelf of the Gulf of Chiriqui, including CC.

In terms of monthly SST climatologies, R7 and CP track closely (see figure 5, left panel from Herrera Carmona et al. 2002). The largest differences occur during February and March, when CP is cooler by as much as 0.7 °C. This may be due largely to the fact that CP is in the middle of the region where wind-driven upwelling is strongest, whereas R7 represents an average over the region. The R6 and EC are significantly different in terms of absolute values, with EC typically being 2.5–3.5 °C higher than R6. However, both show relatively little seasonality. The R4 and CC show similar seasonality, with cooler temperatures from January through March and warmer temperatures the rest of the year. However, CC tends to be significantly cooler (by 0.5–1.5 °C) than RC during

those winter months and slightly warmer (0.3–0.8 °C) for most of the rest of the year.

In terms of Chl-*a* (see Herrera Carmona et al. 2002, Figure 5, right panel), the general seasonal trend at R7 tracks fairly closely with CP, as expected, with maximal values occurring in January through April, although the R7 values are typically 30% (and up to 75%) higher than those assessed at CP. The seasonal pattern for R6 and for R4 is actually very similar to R7 and CP, with CP being typically about 20% larger than R6. On the other hand, results at EC and CC are quite different from R6 and R4, respectively. By way of example, for February the climatological mean for R6 is roughly 1.54 mg m^{-3} , while at EC it is 0.47 mg m^{-3} . The Chl-*a* value peaks in February for R6, while for EC it peaks in April at 0.63 mg m^{-3} (at R6 it has decreased to roughly 0.98 mg m^{-3}). Similarly, at R4 the climatological mean peaks at around 0.69 mg m^{-3} in February/March, during which Chl-*a* is low at CC ($\sim 0.28 \text{ mg m}^{-3}$). At CC, the climatological value peaks in May at roughly 0.42 mg m^{-3} , with the value for R4 being comparable (0.45 mg m^{-3}). There is also a suggestion of a second modest peak in Chl-*a* at CC in October that does not show in R4.

In summary, the climatological values for SST and Chl-*a* for R6 (Herrera Carrera et al. 2022) and for CP are both quite consistent in terms of trends, although the actual magnitudes depend on the averaging area. The R7 data may well be better for characterizing annual variations in the Gulf

of Panama because of the larger spatial averaging. On the other hand, we believe that climatological values for EC and for CC are more reflective of conditions in the western half of the continental shelf along Pacific Panama (and, in particular, the environment around Coiba Island) than those values for R6 and R4, respectively. The latter two regions span a much wider geographical area than Pacific Panama, so a lot of local variability is likely to be smoothed out.

The anomalously high, satellite-derived Chl-*a* values during May 2007 and June 2008 are perhaps the most surprising result from this study. The notable reduction in relative reflectance at 488 nm during these periods is certainly consistent with what one might expect, as Chl-*a* absorbs blue wavelengths. Nevertheless, it remains unclear what caused these events. While local winds were somewhat stronger in May 2007 than typical for that time of year, they appear to have been blowing towards shore, which would suggest initially pushing surface waters towards shore (e.g. downwelling). If the winds remained steadily blowing to the north and north-northeast, surface waters may have flowed alongshore to the east. If the mixed layer had been quite shallow at the time, perhaps there was sufficient wind mixing to carry some nutrients into the mixed layer. However, the winds during May and June 2008 were relatively weak. There also appears no strong evidence of nutrient injection due to high runoff during either May 2007 or June 2008, based on the precipitation data. Corredor-Acosta et al. (2020) suggested other potential reasons for enhanced nutrient concentrations that can lead to increases in Chl-*a*, such as localized upwelling centers and the geostrophic circulation field, but we have little information on these factors in the present study. D’Croz and O’Dea (2007) postulated that the movement of small pockets of cool, deep, nutrient-rich waters onto the shelf and up into the upper layers may represent important events for primary production in the Gulf of Chiriqui, but that it did not appear to be connected to the wind-induced upwelling in the Gulf of Panama.

Without either direct, independent observations to validate the high, satellite-derived Chl-*a* estimates for May 2007 and 2008 or a deeper understanding of the reasons why anomalously large phytoplankton blooms may have been triggered, we are reticent to put complete faith in those estimates. That said, we also have no compelling case to ignore them entirely. Certainly, the challenge is exacerbated by the lack of a long term, *in situ* observational capacity in the Coiba Island/Gulf of Chiriqui region. The establishment and expansion of the Coiba AIP scientific station, along with improvements to satellite-based and model-based data products, may well provide an excellent platform from which to address such events in the future.

ACKNOWLEDGEMENTS

Partial funding for GC and MM was provided through Ontario Tech University internal funds.

Author contributions

Greg Crawford: provided conceptualization, methodology, formal analysis, and writing the original draft. Matthew Mepstead: provided software development, visualization and reviewing-editing. Edgardo Díaz-Ferguson: assisted with conceptualization, funding acquisition (including support for Greg Crawford to present preliminary results at COLACMAR 2022), and reviewing-editing.

REFERENCES

- ACKER JG, LEPTOUKH G. 2007. Online analysis enhances use of NASA earth science data. *Eos Trans.* 88 (2): 14-17. DOI: <https://doi.org/10.1029/2007EO020003>
- ALVARADO J, GUZMÁN H, BREEDY O. 2012. Dis-

- tribution and diversity of echinoderms in the islands of the Gulf of Chiriqui, Panama. *Rev Bio Mar Oceanogr.* 47 (1):13-22.
- AMADOR JA, ALFARO EJ, LIZANO OG, MAGANA VO. 2006. Atmospheric forcing of the eastern tropical Pacific: a review. *Prog Oceanogr.* 60: 101-142.
- AMADOR, JA, DURAN-QUESADA, AM, MORA, G, SAENZ, F, CALDERON, B, MORA, N. 2016a. The easternmost tropical Pacific. Part II: seasonal and intraseasonal modes of atmospheric variability. *Rev Biol Trop.* 64 (1): 23-57. DOI: <https://doi.org/10.15517/rbt.v64i1.23409>
- AMADOR, JA, RIVERA, ER, DURAN-QUESADA, AM, MORA, G, SAENZ, F, CALDERON, B, MORA, N. 2016b. The easternmost tropical Pacific. Part I: a climate review. *Rev Biol Trop.* 64 (1): 1-22. DOI: <https://doi.org/10.15517/rbt.v64i1.23407>
- BALLANCE LT, PITMAN RL, FIEDLER PC. 2006. Oceanographic influences on seabirds and cetaceans of the eastern tropical Pacific: a review. *Prog Oceanogr.* 69: 360-390.
- BRUGNOLI OLIVERA E, MOLINA L, TILL, I, CAMARENA M, MORALES-RAMÍREZ A, DÍAZ-FERGUSON E. 2023. Mesozooplankton and oceanographic conditions in the North zone of Coiba National Park (Panamá, Central America). *Reg Stud Mar Sci.* 66: 103136. DOI: <https://doi.org/10.1016/j.rsma.2023.103136>
- CAMILLI R, PIZARRO O, CAMILLI L. 2007. Rapid swath mapping of reef ecology and associated water column chemistry in the Gulf of Chiriqui, Panama. *Proceedings of MTS/IEEE Oceans 2007.* Vancouver: Institute of Electrical and Electronics Engineers. p. 1-8. DOI: <https://doi.org/10.1109/OCEANS.2007.4449413>
- CAMILLI L, PIZARRO O, CAMILLI R. 2008. Advancing spatial-temporal continuity in coral reef ecosystem pattern detection: the morphology, distribution and chemical environments of coral habitats encompassing Coiba National Park, Panamá. *Proceedings of the 11th International Coral Reef Symposium; 2008 July 7-11.* Ft. Lauderdale, FL, Davie, FL: Nova Southeastern University National Coral Reef Institute. p. 515-519.
- CARDONA V, BRUGNOLI E, DÍAZ-FERGUSON E, MORALES A. 2021. Biología y métodos del estudio del zooplankton gelatinoso con énfasis en investigaciones del Pacífico Este Tropical. *Tecnociencia.* 23 (2): 273-300.
- CHAIGNEAU A, ABARCA DEL RIO R, COLAS FRANCOIS. 2006. Lagrangian study of the Panama Bight and surrounding regions. *J Geophys Res.* 111: C09013. DOI: <https://doi.org/10.1029/2006JC003530>
- COLLEY SB, GLYNN PW, MAY AS, MATE JL. 2006. Species-dependent reproductive responses of eastern Pacific corals to the 1997-1998 ENSO event. *Proceedings of the 10th International Coral Reef Symposium.* p. 61-70.
- CORREDOR-ACOSTA A, CHONG NC, ACOSTA A, PIZARRO-KOCH M, VARGAS A, MEDELLIN-MORA J, SALDIAS GS, ECHEVERRY-GUERRA V, GUTIERREZ-FUENTES J, BETANCUR-TURIZO S. 2020. Spatio-temporal variability of chlorophyll-a and environmental variables in the Panama Bight. *Remote Sens.* 12: 2150. DOI: <https://doi.org/10.3390/rs12132150>
- CORREDOR-ACOSTA A, GASPAS P, CALMETTES B. 2001. Variation in the surface current in the Panama Bight during El Niño and La Niña events from 1993 to 2007. *Bol Invest Mar Cost.* 40: 33-56.
- D'CROZ L, MATE JL, OKE JE. 2001. Responses to elevated sea water temperature and UV radiation in the coral *P. lobate* from upwelling and non-upwelling environments on the Pacific coast of Panama. *Bull Mar Sci.* 69 (1): 203-214.
- D'CROZ L, O'DEA A. 2007. Variability in upwelling along the Pacific shelf of Panama and implications for the distribution of nutrients and chlorophyll. *Estuar Coast Shelf Sci.* 73: 325-340.
- D'CROZ L, ROBERTSON DR. 1997. Coastal oceanographic conditions affecting coral reefs on both sides of the Isthmus of Panama. *Proceedings of the 18th International Coral Reef Symposium.* 2 (205): 2053-2058.

- DEVIS-MORALES A, SCHNEIDER W, MONTOYA-SANCHEZ RA, RODRIGUEZ-RUBIO E. 2008. Monsoon-like winds reverse oceanic circulation in the Panama Bight. *Geophys Res Lett.* 35: L20607. DOI: <https://doi.org/10.1029/2008GL035172>
- ENRIGHT SG, MENESES-ORELLANA R, KEITH I. 2021. The Eastern Tropical Pacific Marine Corridor (CMAR): the emergence of a voluntary regional cooperation mechanism for the conservation and sustainable use of marine biodiversity within a fragmented regional ocean governance landscape. *Front Mar Sci.* 8:674825. DOI: <https://doi.org/10.3389/fmars.2021.674825>
- FERNANDEZ-ÁLAMO MA, FARBER-LORDA J. 2006. Zooplankton and the oceanography of the eastern tropical Pacific: a review. *Prog Oceanogr.* 69: 318-359.
- FIEDLER PC, TALLEY LD. 2006. Hydrography of the eastern tropical Pacific: a review. *Prog Oceanogr.* 69: 143-180.
- GARCIA-FRANCO, JL, CHADWICK, R, GRAY, LJ, OSPREY, S, ADAMS, DK. 2023. Revisiting mechanisms of the Mesoamerican Midsummer drought. *Climate Dyn.* 60: 549-569. DOI: <https://doi.org/10.1007/s00382-022-06338-6>
- [GMAO] GLOBAL MODELING AND ASSIMILATION OFFICE. 2015. MERRA-2 `tavgM_2d_flux_Nx`: 2d, monthly mean, time-averaged, single-level, assimilation, surface flux diagnostics V5.12.4. Greenbelt: Goddard Earth Sciences Data and Information Services Center. [accessed 2023 May 25]. DOI: <https://doi.org/10.5067/0JRLVL8YV2Y4>
- GUZMÁN HM, BEAVER CE, DÍAZ-FERGUSON E. 2021. Novel insights into the genetic population connectivity of transient whale sharks (*Rhincodon typus*) in Pacific Panama provide crucial data for conservation efforts. *Front Mar Sci.* 8: 744109. DOI: <https://doi.org/10.3389/fmars.2021.744109>
- HARVEY ET, KRATZER S, PHILIPSON P. 2015. Satellite-based water quality monitoring for improved spatial and temporal retrieval of chlorophyll-*a* in coastal waters. *Rem Sense Env.* 158: 417-430. DOI: <https://doi.org/10.1016/j.rse.2014.11.017>
- HERRERA CARMONA JC, SELVARAJ JJ, GIRALDO A. 2022. Dynamic regionalization of the Panama Bight, Eastern Tropical Pacific, using remote sensing data. *Int J Remote Sens.* 43 (9): 313103151. DOI: <https://doi.org/10.1080/01431161.2022.2063040>
- HU C, FENG L, LEE Z, FRANZ BA, BAILEY SW, WERDELL PJ, PROCTOR CW. 2019. Improving satellite global chlorophyll *a* data products through algorithm refinement and data recovery. *J Geophys Res.* 124: 1524-1543. DOI: <https://doi.org/10.1029/2019JC014941>
- HU S, FEDOROV AV. 2019. The extreme El Niño of 2015-2016: the role of westerly and easterly wind bursts, and preconditioning by the failed 2014 event. *Climate Dyn.* 52: 7339-7357. DOI: <https://doi.org/10.1007/s00382-017-3531-2>
- HUFFMAN GJ, STOCKER EF, BOLVIN DT, NELKIN EJ, JACKSON T. 2023. GPM IMERG Final Precipitation L3 1 day 0.1 degree x 0.1 degree V07, Greenbelt, MD, Goddard Earth Sciences Data and Information Services Center (GES DISC). [accessed 2023 Sep 14]. DOI: <https://doi.org/10.5067/GPM/IMERGDF/DAY/07>
- JIANG W, KNIGHT BR, CORNELISEN C, BARTER P, KUDELA R. 2017. Simplifying regional tuning of MODIS algorithms for monitoring chlorophyll-*a* in coastal waters. *Front Mar Sci.* 4: 151. DOI: <https://doi.org/10.3389/fmars.2017.00151>
- KESSLER WS. 2006. The circulation of the eastern tropical Pacific: a review. *Prog Oceanogr.* 69: 181-217.
- LAVIGNE H, VAN DER ZANDE D, RUDDICK K, CARDOSO DOS SANTOS JF, GOHIN F, BROTA V, KRATZER S. 2021. Quality-control tests for OC4, OC5 and NIR-red satellite chlorophyll-*a* algorithms applied to coastal waters. *Rem Sens Env.* 255: 112237. DOI: <https://doi.org/10.1016/j.rse.2020.112237>
- MATÉ J, TOVAR D, ARCIA E, HIDALGO Y. 2009. Plan de manejo del Parque Nacional Coiba. Autori-

- dad Nacional del Ambiente. 160 p.
- MESTAS-NUNEZ AM, MILLER AJ. 2006. Interdecadal variability and climate change in the eastern tropical Pacific: a review. *Prog Oceanogr.* 69: 267-284.
- [NASA OBPB] THE NATIONAL AERONAUTICS AND SPACE ADMINISTRATION OCEAN BIOLOGY PROCESSING GROUP. 2019a. MODIS Aqua Level 3 SST Thermal IR Daily 4km Daytime V2019.0. California: Physical Oceanography Distributed Active Archive Center (PO.DAAC). [accessed 2023 May 25]. DOI: <https://doi.org/10.5067/MODSA-1D4D9>
- [NASA OBPB] THE NATIONAL AERONAUTICS AND SPACE ADMINISTRATION OCEAN BIOLOGY PROCESSING GROUP. 2019b. MODIS Aqua Level 3 SST MID-IR Monthly 4km Nighttime V2019.0. California: Physical Oceanography Distributed Active Archive Center (PO.DAAC). [accessed 2023 May 25]. DOI: <https://doi.org/10.5067/MODAM-MO4N9>
- [NASA OBPB] THE NATIONAL AERONAUTICS AND SPACE ADMINISTRATION OCEAN BIOLOGY PROCESSING GROUP. 2022. Moderate-resolution Imaging Spectroradiometer (MODIS) Aqua Chlorophyll Data; 2022 reprocessing. Greenbelt: NASA Ocean Biology Distributed Active Archive Center (OB.DAAC). [accessed 2023 May 25]. DOI: <https://doi.org/10.5067/AQUA/MODIS/L3M/CHL/2022>
- O'REILLY JE, WERDELL PJ. 2019. Chlorophyll algorithms for ocean color sensors - OC4, OC5 & OC6. *Rem Sens Env.* 229: 32-47.
- PAWLOWICZ R. 2021. M_Map: a mapping package for MATLAB, version 1.4n. <https://www.eoas.ubc.ca/~rich/map.html>.
- PENNINGTON JT, MAHONEY KL, KUWAHARA VS, KOLBER DD, CALIENES R, CHAVEZ FP. 2006. Primary production in the eastern tropical Pacific: a review. *Prog Oceanogr.* 69: 285-317.
- PODESTA GP, GLYNN PW. 1997. Sea surface temperature variability in Panama and Galapagos: extreme temperatures causing coral bleaching. *J Geophys Res.* 102 (C7): 15749-15759.
- RODRIGUEZ-RUBIO E, STUARDO J. 2002. Variability of photosynthetic pigments in the Colombian Pacific Ocean and its relationship with the wind field using ADEOS-I data. *Proc Indian Acad Sci (Earth Planet Sci)*. 111 (3): 227-236.
- RODRIGUEZ-RUBIO E, SCHNEIDER W, ABERCA DEL RIO R. 2003. On the seasonal circulation within the Panama Bight derived from satellite observations of wind, altimetry and sea surface temperature. *Geophys Res Lett.* 30 (7): 1410. DOI: <https://doi.org/10.1029/2002GL016794>
- SANTOSO, A, MCPHADEN MJ, CAI W. 2017. The defining characteristics of ENSO extremes and the strong 2015/2016 El Niño. *Rev Geophys.* 55: 1079-1129. DOI: <https://doi.org/10.1002/2017RG000560>
- SMAYDA TJ. 1966. A quantitative analysis of the phytoplankton of the Gulf of Panama. III. General ecological conditions and the phytoplankton dynamics at 8° 45' N, 79° 23' W from November 1954 to May 1957. *Inter-American Tropical Tuna Commission Bulletin.* 11: 353-612.
- TILSTONE GH, LOTLIKER AA, MILLER PI, ASHRAF PM, KUMAR TS, SURESH T, RAGAVAN BR, MENON HB. 2013. Assessment of MODIS-Aqua chlorophyll-a algorithms in coastal and shelf waters of the eastern Arabian Sea. *Cont Shelf Res.* 65: 14-265. DOI: <https://doi.org/10.1016/j.csr.2013.06.003>
- THE MATHWORKS INC. 2022. MATLAB version: 9.13.0 (R2022b), Natick, Massachusetts: The MathWorks Inc. <https://www.mathworks.com>.
- WANG C, FIEDLER PC. 2006. Eddies and tropical instability waves in the eastern tropical Pacific: a review. *Prog Oceanogr.* 69: 218-238.
- WILLETT CS, LEBEN RR, LAVIN MF. 2006. ENSO variability and the eastern tropical Pacific: a review. *Prog Oceanogr.* 69: 239-266.
- WYRTKI K. 1966. Oceanography of the eastern equatorial Pacific Ocean. *Oceanogr Mar Biol Ann Rev.* 4: 33-68.

